

Lipid Lateral Diffusion in Ordered and Disordered Phases in Raft Mixtures

Andrey Filippov, Greger Orädd, and Göran Lindblom

Department of Biophysical Chemistry, Umeå University, SE-901 87 Umeå, Sweden

ABSTRACT Lipid lateral diffusion coefficients in the quaternary system of dioleoylphosphatidylcholine (DOPC), sphingomyelin, cholesterol, and water were determined by the pulsed field gradient NMR technique on macroscopically aligned bilayers. The molar ratio between dioleoylphosphatidylcholine and sphingomyelin was set to 1:1, the cholesterol content was varied between 0 and 45 mol %, the water content was 40 wt %, and the temperature was varied between 293 and 333 K. The diffusion coefficients were separated into fast and slow spectral components by using the CORE method for global analysis of correlated spectral data. A large two-phase region, tentatively assigned to the liquid disordered (l_d) and the liquid ordered (l_o) phases, was present in the phase diagram. The l_d phase was enriched in dioleoylphosphatidylcholine and exhibited diffusion coefficients that were about three to five times larger than for the l_o phase. Both the diffusion coefficients and the apparent activation energies for the quaternary systems were compatible with earlier reports on ternary phospholipid/cholesterol/water systems. However, in contrast to the latter ternary systems, the exchange of lipids between the l_o and the l_d phases was slow on the timescale for the diffusion experiment for the quaternary ones. This means that on the millisecond timescale fluid, ordered domains are floating around in a sea of faster diffusing lipids, assigned to consist of mainly dioleoylphosphatidylcholine.

INTRODUCTION

Many recent studies have revealed that cell membranes possess a rather complex lateral organization. The existence of domains in membranes, referred to as lipid rafts, that are rich in cholesterol (CHOL), is a central area of research in lipid biology (Brown, 1998; Rietveld and Simons, 1998; Simons and Ikonen, 1997). Rafts are proposed to play a dominant role in signal transduction, lipid trafficking, and transcytosis (Simons and Toomre, 2000; Simons and van Meer, 1988). Evidence for lipid domain formation was first claimed by the discovery of the so-called detergent resistant membranes (DRM) that could withstand solubilization by cold Triton X-100 (Brown, 1998). DRMs were enriched in CHOL and the mainly saturated lipid sphingomyelin (SM), whereas the remainder of the membrane contained more of unsaturated lipids, mainly phosphatidylcholines (PCs). The possible existence of DRMs has stimulated a great deal of lipid research; in particular, much effort has been put on investigations of the role played by CHOL in the formation and function of rafts.

By utilizing a variety of physical techniques, lipid domains were observed in simple model membrane systems, consisting of either multibilayer lipid systems, lipid monolayers, or lipid (giant) vesicles. The methods used include atomic force microscopy (Lawrence et al., 2003; Rinia et al., 2001; Yuan et al., 2002), fluorescence microscopy (Dietrich et al., 2001; Samsonov et al., 2001; Veatch and Keller, 2002), fluorescence quenching (Ahmed et al., 1997), single particle tracking (Dietrich et al., 2001), differential scanning calorimetry

(Gandhavadi et al., 2002; Shaikh et al., 2001), electron spin resonance and infrared spectroscopy (Veiga et al., 2001), and x-ray diffraction (Gandhavadi et al., 2002). Most of these studies were concentrated on systems, in which low- and high-melting lipids were present in equal fractions, together with varying fractions of CHOL. A generic phase diagram for such systems was recently proposed (Veatch and Keller, 2003). Such a basic phase diagram is of great importance to get a good understanding of the driving forces behind the domain formation in lipid bilayer systems. In fact, it seems that most relevant lipid systems published so far show a similar phase behavior to the one first published for the ternary system of dipalmitoylphosphatidylcholine, CHOL, and water (Vist and Davis, 1990). In this phase diagram it was discovered that so-called liquid ordered (l_o) and liquid disordered (l_d) phases formed in equilibrium with each other. Both these phases are in a fluid liquid crystalline state, but the hydrocarbon chains in the l_o phase are more highly ordered than those in the l_d phase. The phase diagram exhibits a large two-phase area with the l_o and the l_d phases (Ipsen et al., 1987; Vist and Davis, 1990). Recently, the phase diagrams for systems of other saturated and mono-unsaturated phospholipids and CHOL were shown to have a similar appearance as those above, if differences in the main transition, T_m , for the lipids are accounted for (Filippov et al., 2003a,b; Thewalt and Bloom, 1992). Thus, DRMs were believed to be made up of such an l_o phase structure.

To gain a more elaborate understanding of the dynamics in raft systems, we have determined the lateral diffusion of the different compounds building up these systems (Filippov et al., 2003a,b; Orädd et al., 2002). The l_o phase was characterized with respect to the lipid lateral diffusion in ternary systems, and it was shown that the diffusion coefficient was typically 2–3 times slower in the l_o phase than in the l_d phase. In this work we extended our investigations to include the

Submitted June 18, 2003, and accepted for publication September 24, 2003.

Address reprint requests to Greger Orädd, Tel.: +46-90-786-53-67; E-mail: greger.oradd@chem.umu.se.

© 2004 by the Biophysical Society

0006-3495/04/02/891/06 \$2.00

quaternary system of dioleoylphosphatidylcholine (DOPC), SM, CHOL, and water, where the water content was kept constant at 40 wt %.

MATERIALS AND METHODS

Preparation of oriented samples

The following substances were used for the preparation of macroscopically aligned lipid bilayers: 1,2-dioleoyl-*sn*-glycero-3-phosphocholine (DOPC; Avanti Polar Lipids, Birmingham, AL), chicken egg yolk sphingomyelin, ~99% (SM; Sigma, St. Louis, MO), and 5-cholesten-3 β -ol, Sigma grade: 99+ % (CHOL; Sigma, St. Louis, MO). Deuterated water ($^2\text{H}_2\text{O}$, 99.7%) was purchased from Larodan AB, Malmö, Sweden.

The samples were prepared with a molar ratio (DOPC/SM/CHOL) of 1:1: n_C , where n_C was varied from 0 to 1.66, corresponding to CHOL concentrations (X) of 0, 8, 15, 19, 24, 29, 33, 39, and 45 mol %.

Appropriate amounts of lipids and CHOL were dissolved in chloroform at a concentration of 15 mg/mL. For the 100-MHz instrument, 25 μL of the solution was put onto each of 60 glass plates ($5 \times 14 \text{ mm}^2$) and for the 400-MHz instrument, the corresponding amount was 13 μL onto 35 plates ($2.3 \times 14 \text{ mm}^2$). The solvent was evaporated at atmospheric pressure and then under vacuum at 303 K for 6 h. The glass plates were stacked and placed in a humid $^2\text{H}_2\text{O}$ atmosphere in which the hydrated bilayers formed. Finally, an excess of $^2\text{H}_2\text{O}$ was added with a syringe to obtain 40 wt % $^2\text{H}_2\text{O}$ in all samples before they were sealed. This procedure ensured that the membranes were kept at maximal hydration also at elevated temperatures.

The degree of orientation varied from 50% to 95%, as determined from the ^{31}P NMR lineshape. The obtained diffusion coefficients did not depend on the degree of orientation.

Pulsed field gradient (pfg) NMR

The majority of the proton diffusion measurements were performed on a Chemagnetics Infinity (Varian, Fort Collins, CO) spectrometer operating at a proton frequency of 100 MHz. Some measurements were also performed on a similar system operating at 400 MHz. Both spectrometers have purpose-built goniometer probes that enable samples of macroscopically aligned bilayers to be oriented with the bilayer normal at the magic angle with respect to the main magnetic field. The temperature was controlled within $\pm 0.5^\circ\text{C}$ by a heated air stream passing the sample. The calibration of the temperature was checked by measuring the frequency separation of the two peaks in a sample of ethylene glycol. Details of the pfg-NMR method for lipid lateral diffusion measurements can be found elsewhere (Lindblom and Orädd, 1994; Orädd and Lindblom, 2003, 2004). For all measurements the stimulated echo (STE) pulse sequence was used in which the echo amplitude attenuation due to diffusion is given by (Tanner, 1970):

$$A = A_0 \exp\left(-\gamma^2 \delta^2 g^2 D \left(\Delta - \frac{\delta}{3}\right)\right), \quad (1)$$

where A_0 is the echo amplitude without applied gradients, γ is the gyromagnetic ratio, Δ is the time interval between gradient pulses, and δ and g are the duration and amplitude of the pulsed field gradients, respectively. The initial echo amplitude A_0 was determined by the longitudinal and transverse NMR relaxation times according to Tanner (1970):

$$A_0 = \frac{I}{2} \times \exp\left(\frac{-2 \cdot \tau}{T_2}\right) \times \exp\left(-\frac{T}{T_1}\right), \quad (2)$$

where I is the factor proportional to the proton content in the system, T_1 and T_2 are the longitudinal and transverse NMR relaxation times, and τ and T are the time intervals determining transverse and longitudinal relaxation, respectively (Lindblom and Orädd, 1994).

In the case of biexponential decays, the data were fitted to an equation with two diffusion coefficients:

$$A = A_1 \exp\left(-\gamma^2 \delta^2 g^2 D_1 \left(\Delta - \frac{\delta}{3}\right)\right) + A_2 \exp\left(-\gamma^2 \delta^2 g^2 D_2 \left(\Delta - \frac{\delta}{3}\right)\right). \quad (3)$$

This would be the case for a system consisting of two phases with slow exchange, as compared to the diffusion time. In this case the relative populations of lipids in the two phases can be extracted directly from the preexponential coefficients, A_1 and A_2 , if relaxation effects can be neglected. If the relaxation in one of the phases is much faster than in the other, the preexponential coefficient will be diminished and might be too small to be detected, so that the observed decay will be apparent monoexponential.

If the exchange rate between two phases is comparable to the diffusion time, the decay will follow an equation similar to Eq. 3, but in this case both the preexponential factors and the apparent diffusion coefficients will be functions of the diffusion coefficients, relative populations, lifetimes, and NMR relaxation in the two phases (Kärger et al., 1988). This means that the resulting preexponential factors and apparent diffusion coefficients will in general depend on the conditions under which the experiment is performed.

Finally, if the exchange rate is much faster than the diffusion time, the observed decay will be monoexponential with an apparent diffusion coefficient, which is a population weighted average from the two phases.

In the diffusion experiments only δ (100-MHz instrument) or g (400-MHz instrument) was varied, keeping all other parameters constant. The starting value of the varied parameters was chosen so that the residual signal from water was completely suppressed to observe only the signal from the lipids. Eventually, at the end of the experiment also the lipid signal was completely suppressed. The following parameter settings were used: $g = 1.15 \text{ T/m}$, and δ varied from 1 to 12 ms for the 100-MHz instrument; and $\delta = 5 \text{ ms}$, and g varied from 0.6 to 6.0 T/m for the 400-MHz instrument. The diffusion time was varied in the interval from 50 to 250 ms, with the majority of the experiments made at 200 ms. The number of accumulated scans ranged from 128 to 256 for the 100-MHz instrument and from 64 to 160 for the 400-MHz instrument. The total time for a diffusion experiment took between 30 and 150 min.

Data analysis

A simple analysis based on peak heights or integrated intensities clearly showed the presence of more than one diffusion coefficient in several samples. To separate the bandshapes corresponding to the slow and fast diffusion components we decided to use the CORE method for global analysis of the entire data set (Stilbs and Paulsen, 1996; Stilbs et al., 1996). This method is based on a two-level fitting routine, in which the lower level fits each individual frequency channel intensity to the chosen equation, i.e., Eq. 1 or Eq. 3. The resulting global error square sum from this fit was then passed on to the higher level fitting routine, in which the diffusion coefficient(s) was (were) varied and the result was sent back to the lower level. This is repeated until convergence was achieved at the higher level. The output from the CORE analysis was the fitted values of the diffusion coefficients together with the individual amplitudes of the diffusion components for each frequency channel, i.e., the individual bandshapes of the diffusional components. For each experimental set of data the CORE routine was applied, first using Eq. 1, and then using Eq. 3. The distinction between whether there were one or two components was judged from a significant improvement in the normalized global error square sum, when using one or two components in the fit.

An example of the CORE analysis is presented in Fig. 1 for a sample with 29 mol % CHOL at 308 K. The data were collected on the 400-MHz instrument, but the data are also representative for the 100-MHz instrument, both with respect to the signal-to-noise level and magnitude of the residuals. In this experiment the following parameters were used: $\tau = 10 \text{ ms}$, $T = 50 \text{ ms}$, $\delta = 5 \text{ ms}$, $g = 0.6\text{--}6.0 \text{ T/m}$, $\Delta = 60 \text{ ms}$; and the resulting diffusion coefficients were 5.0 and $1.0 \times 10^{-12} \text{ m}^2/\text{s}$. The top panel shows the

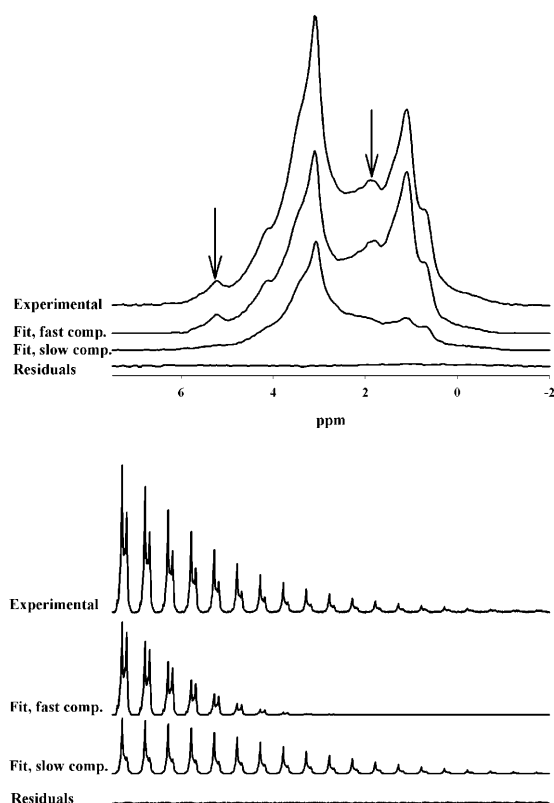


FIGURE 1 (Top) The first spectrum from the CORE analysis for a pfg-NMR experiment acquired on the 400-MHz instrument for a sample with 29 mol % CHOL. The temperature is 308 K. The arrows indicate spectral features observed only in the spectrum of DOPC. (Bottom) Stackplot of all spectra obtained in the same experiment as (top). In this experiment the following parameters were used: $\tau = 10$ ms, $T = 50$ ms, $\delta = 5$ ms, $g = 0.6$ – 6.0 T/m, $\Delta = 60$ ms, and the resulting diffusion coefficients were 5.0 and 1.0×10^{-12} m²/s.

spectrum from the experiment with the lowest gradient, together with the bandshapes of the two diffusion components obtained from the CORE analysis. The bottom trace displays the difference between the fit and the experimental spectrum. In the lower panel all 19 experiments in the diffusion determination are stacked to show the decays of the spectrum on increasing values of g .

To estimate the error in the measurements, data analysis was also performed, using other nonlinear fitting routines on the peak intensity of the dominant peak as well as on the integral of the complete spectrum. For none of the samples did the results from the three methods differ by more than 5%. A conservative estimate of the measurement error would thus be $\pm 5\%$ of the obtained diffusion (D).

In the pfg-NMR method employed here, the field gradient was along the main magnetic field. Since the lipid diffusion occurred only within the plane of the bilayer, only the component of the gradient that was parallel to the bilayer plane gave rise to the echo attenuation. Thus, the effective gradient will be $g_{\text{eff}} = g \sin 54.7^\circ$, and the diffusion coefficient obtained will need to be multiplied by a factor of 1.5 to obtain the lateral diffusion coefficient; $D_L = 1.5 \times D$ (Orädd and Lindblom, 2004; Wästerby et al., 2002).

RESULTS

A partial phase diagram was obtained by varying the temperature and the CHOL concentration, and performing a

CORE analysis that gave one or two diffusion coefficients (Fig. 2), represented by the filled and open circles, respectively. Some cases were difficult to classify, either because different measurements gave different results, or because the improvement in the error sum was intermediate between the one- and two-component categorization. These points, situated in the border region, are represented by thick-line circles in Fig. 2.

Fig. 3 illustrates the typical lineshapes obtained on the 100-MHz instrument in one- and two-component CORE fits of the data at 318 K for different CHOL contents. At $X = 0$, there was only one (fast) component; at $X = 7.5$, 15, and 24, the analysis yielded two components, one fast (solid line) and one slower (dashed line); whereas at $X = 33$ and 45, only one (slow) component was present. Both the slow and fast diffusing components displayed two dominant peaks, corresponding to the methylenes of the acyl chain at 1.1 ppm, and to the methyl-groups of the choline headgroup at 3.1 ppm. Due to the rather poor spectral resolution obtained in this kind of experiment, especially for the 100-MHz instrument, it was difficult to separate the signals from the two lipid species. However, in experiments performed at 400 MHz, some characteristic features in the spectrum for DOPC could be partly resolved, namely, the signals at 5.2 and 2.0 ppm originating from the $-\text{CH}_2-\text{CH}=\text{CH}-\text{CH}_2-$ protons of the unsaturated chains. These signals could be observed in the experimental spectrum and, moreover, only for the component exhibiting fast diffusion (Fig. 1). No signal was obtained from CHOL, due to the fast spin-spin relaxation for this rather rigid molecule (Orädd et al., 2002).

Fig. 4 summarizes all the results for the dependence of the slow and fast components on the CHOL content at four different temperatures. For comparison, data for the systems with DOPC/CHOL/water and SM/CHOL/water at the same temperatures are also shown as solid and dashed lines, respectively.

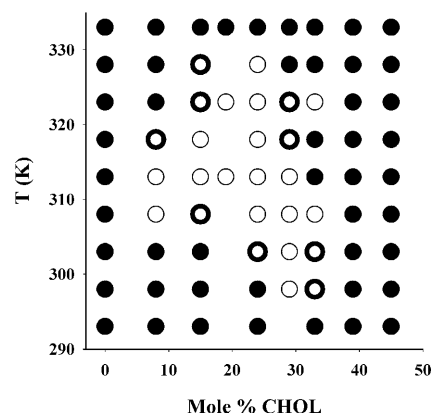


FIGURE 2 An overview of the studied system. The circles denote measured points and are classified according to whether the diffusion decay was monoexponential (closed) or biexponential (open). Points that were difficult to classify are shown as open circles with thick lines.

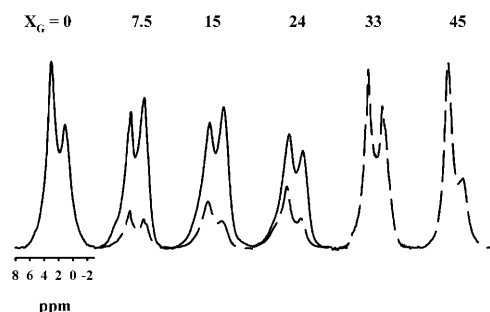


FIGURE 3 Spectral components according to the CORE analysis for samples with various CHOL contents at 318 K. The measurement was performed on the 100-MHz instrument with the following parameters: $\tau = 14$ ms, $T = 190$ ms, $\delta = 1\text{--}12$ ms, $g = 1.15$ T/m, $\Delta = 204$ ms. The fast diffusion component is shown with solid lines and the slow component with dashed lines. The numbers above each spectrum indicate the mol % of CHOL in each sample.

DISCUSSION

The possible formation of domains of a liquid-ordered phase, “rafts”, in bilayers now seems to be widely accepted (Ahmed et al., 1997; Dietrich et al., 2001; Gandhavadi et al., 2002; Hao and Chen, 2001; Rinia et al., 2001; Samsonov et al., 2001; Shaikh et al., 2001; Veatch and Keller, 2002, 2003; Veiga et al., 2001; Yuan et al., 2002). Recently, a generic miscibility phase diagram for ternary raft-forming mixtures was proposed (Veatch and Keller, 2003). Such a diagram typically contains 1:1 mixtures of an unsaturated and a saturated lipid, such as PC or SM, and various fractions of CHOL. The diagram displays an upper miscibility temperature that is fairly constant for CHOL contents between 10 and 30 mol %, and then decreases rapidly as the CHOL concentration is further increased. A comparison between the phase diagram by Veatch and Keller and the diagram in our Fig. 2 strongly indicates that the two-

component diffusion behavior observed in our study is a consequence of the lateral separation into an l_o phase, enriched in CHOL and SM, and an l_d phase, containing mostly DOPC. The CHOL concentration, at which the miscibility temperature starts to drop, seems to correlate better with the results obtained by fluorescence spectroscopy on giant lipid vesicles (Veatch and Keller, 2003) than the data obtained from atomic force microscopy (AFM) (Rinia et al., 2001), where lipid domains were observed for CHOL contents up to 50 mol %. This difference could be due to effects from the solid support in the AFM measurements (Leidy et al., 2002; Tokumasu et al., 2003). Our measurements were performed on a stack of ~ 1000 bilayers, and therefore the effects from the glass surfaces were negligible. Thus, our studies of lipid domains are more comparable with data from the vesicle systems.

At $X = 0$, corresponding to the ternary DOPC/SM/water system, the diffusion was monoexponential and slightly lower than that for the DOPC/water system (Fig. 4). This was expected since the presence of SM, both in the form of gel patches and mixed into the fluid phase, would decrease the diffusion of DOPC.

As CHOL was added, the system entered the two-phase region, in which the fast diffusion coefficient was similar to that in DOPC/CHOL/water, whereas the curve for the slow diffusion coefficient fairly well resembled that for SM/CHOL/water. This correlates well with the separation into the l_d phase, enriched in DOPC, and the l_o phase, enriched in SM and CHOL.

At $X > 33$, the diffusion decay was again monoexponential with D_L values close to the mean value of D_L found in the DOPC/CHOL/water and SM/CHOL/water systems. The same observation also holds true for $T > 328$ K, where single diffusional decays were observed. This “averaging of D_L ” has been observed also in other systems, both for different lipids (Eriksson and Lindblom, 1993) and for mixtures of lipid and CHOL (Orädd et al., 2002). Thus, we expect that all three lipid components diffuse with the same D_L in this region, although only the phospholipids were actually observed.

Our data can be compared with a recent fluorescence correlation spectroscopy study in a similar system, in which a two-phase region was reported for $10 > X > 33$ at 298 K (Kahya et al., 2003). The values of the fast diffusion coefficient agreed well with those obtained by us; and, for the two CHOL contents for which we observe biexponential decays at 298 K, also the slow diffusion coefficient was in reasonable agreement. The difference in the extension of the two-phase region might be due to the fast transverse spin relaxation in the l_o phase at lower temperatures that effectively removed this component from the diffusional decays. Thus, even though the diffusional decay was monoexponential, we cannot exclude the possibility of a two-phase coexistence in the low-temperature region. The apparent lower miscibility temperature of ~ 300 K for 7.5 to 30 mol %

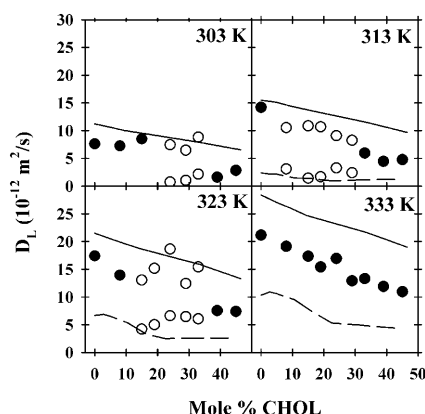


FIGURE 4 Lateral diffusion coefficients obtained as a function of CHOL content at the indicated temperatures. Filled circles: D_L obtained in monoexponential fits. (Open circles) D_L obtained in biexponential fits. (Solid lines) Data for the corresponding ternary DOPC/CHOL/water system. (Dashed lines) Data for the corresponding ternary SM/CHOL/water system.

CHOL (Fig. 2) therefore needs further investigation before it can be firmly established.

The lateral diffusion of lipids in phase-separated l_d/l_o systems has also been studied by observing the motion of colloidal gold particles attached to lipid analogs introduced into the bilayers (Dietrich et al., 2001). In that study the ratio of $D_L(l_d)/D_L(l_o)$ was found to be ~ 3 . This is in agreement with our study (Fig. 4). It should be noticed, however, that although the obtained ratio was similar, the absolute values of $D_L(l_d)$ and $D_L(l_o)$ were ~ 5 times larger in our study. A reasonable explanation for this is the large mass of the incorporated gold particle, resulting in a largely decreased diffusion coefficient for such lipids.

An interesting feature seen in Fig. 4 is the relative independence of D_L on CHOL content, both for the l_d and l_o phases. This feature has also been observed in the ternary systems of DMPC/CHOL/water and the SM/CHOL/water (Almeida et al., 1992; Filippov et al., 2003a). For the l_o phase D_L was even found to increase slightly with CHOL content, and this behavior held true also in the quaternary system (Fig. 4). This increase was explained by the increase of free volume per molecule with increasing CHOL concentration (Almeida et al., 1992; Polson et al., 2001).

The NMR lineshapes of DOPC and SM were quite similar, and, due to the poor resolution (especially on the 100-MHz system), it was impossible to separate the two lipid signals. On the 400-MHz system the resolution was better, and the spectral components obtained from the CORE analysis gave some evidence that DOPC was present mainly in the fast diffusing component. The signals from protons adjacent to the double bonds in DOPC at 5.2 and 2.0 ppm were clearly visible in the spectra. These spectral features were visible only in the fast component spectra obtained from the CORE analysis, and this implies that DOPC was mainly present in the fast component. To thoroughly study the partition of the lipids into the two phases it will be necessary to employ methods that allow the signal from each of the system constituents to be studied separately. Work in this direction has been initiated in our laboratory (Orädd et al., 2002).

If chemical exchange of lipids between the two phases would occur on the same timescale as the diffusion time of the experiments, one would expect that both the preexponential factors and diffusion coefficients would change as the diffusion time is varied (Kärger et al., 1988). In this study τ was kept as short as possible to minimize the T_2 relaxation, and thus preserve as much signal as possible, and T was varied between 30 to 190 ms as the diffusion time, $T + \tau$, was varied. These variations did not alter the relative populations or the diffusion coefficients obtained from the CORE analysis, implying that the exchange of lipids between the l_o and the l_d phases is slow on this timescale, which is in stark contrast to the observed fast exchange seen in the ternary systems (Filippov et al., 2003a,b). Since a lipid in the l_o phase on the average moves $\sim 1 \mu\text{m}$ during 200 ms, the domains must be much larger than $1 \mu\text{m}$ to obtain a slow

exchange. Although reported values of the size of the lipid domains vary a lot, most observations seem to favor rather large domains ($5\text{--}50 \mu\text{m}$), in accordance with our observations. There is also the possibility that different lipids segregate exclusively into different domains. In this case the domain sizes still need to be larger than micrometers to avoid restricted diffusion at the domain boundaries on the used timescales. It should, however, be emphasized that further measurements with extended variations in both the diffusion time and the T_1 and T_2 relaxation times have to be performed before any firm conclusions can be made. In particular, isotopic-enriched molecules will be needed to be able to make a more conclusive statement on the molecular lifetimes in the different phases.

The temperature dependence of D_L was analyzed assuming an Arrhenius-type of diffusion process. It was found that the apparent activation energy, E_A , was $\sim 20\text{--}25 \text{ kJ/mol}$ for the fast diffusion component, whereas it was significantly higher, $45\text{--}65 \text{ kJ/mol}$, for the slow component. A variation in the CHOL concentration did not result in a particular change or trend in the E_A s. The activation energies obtained can be compared with reported E_A s in the ternary systems of SM/CHOL/water, DMPC/CHOL/water, DOPC/CHOL/water, and POPC/CHOL/water, in which E_A was in the range of $30\text{--}40 \text{ kJ/mol}$ for the l_d phase and between $55\text{--}65 \text{ kJ/mol}$ for the l_o phase. Thus, the results correlate well with the general picture of larger E_A s for the l_o phase.

CONCLUSIONS

We have investigated lateral organization in so-called raft mixtures of DOPC/SM/CHOL in 40 wt % $^2\text{H}_2\text{O}$ by the noninvasive pfg-NMR method. The presence of two-phase regions of l_o and l_d phases is manifested in two distinct lateral diffusion coefficients of the lipids as opposed to the single diffusion coefficient observed for the l_d and l_o one-phase areas. The chemical exchange of lipids between domains is found to be slow on the timescale for the measurements of the lateral diffusion. This allows the phase borders of the two-phase region to be mapped out without the need of probe molecules commonly used by other methods. The results are in excellent agreement with previously published results on giant lipid vesicles.

This work was supported by the Swedish Research Council and the Knut and Alice Wallenberg Foundation. A.F. acknowledges financial support from the Royal Swedish Academy of Sciences.

REFERENCES

- Ahmed, S. N., D. A. Brown, and E. London. 1997. On the origin of sphingolipid/cholesterol-rich detergent-insoluble cell membranes: physiological concentrations of cholesterol and sphingolipid induce formation of a detergent-insoluble, liquid-ordered lipid phase in model membranes. *Biochemistry*. 36:10944–10953.

- Almeida, P. F. F., W. L. C. Vaz, and T. E. Thompson. 1992. Lateral diffusion in the liquid phases of dimyristoylphosphatidylcholine/cholesterol bilayers: a free volume analysis. *Biochemistry*. 31:6739–6747.
- Brown, R. E. 1998. Sphingolipid organization in biomembranes: what physical studies of model membranes reveal. *J. Cell Sci.* 111:1–9.
- Dietrich, C., L. A. Bagatolli, Z. N. Volovyk, N. L. Thompson, M. Levi, K. Jacobson, and E. Gratton. 2001. Lipid raft reconstituted in model membranes. *Biophys. J.* 80:1417–1428.
- Eriksson, P. O., and G. Lindblom. 1993. Lipid and water diffusion in bicontinuous cubic phases measured by NMR. *Biophys. J.* 64:129–136.
- Filippov, A., G. Orädd, and G. Lindblom. 2003a. The effect of cholesterol on the lateral diffusion of phospholipids in oriented bilayers. *Biophys. J.* 84:3079–3086.
- Filippov, A., G. Orädd, and G. Lindblom. 2003b. Influence of cholesterol and water content on phospholipid lateral diffusion in bilayers. *Langmuir*. 19:6397–6400.
- Gandhavadi, M., D. Allende, A. Vidal, S. A. Simon, and T. J. McIntosh. 2002. Structure, composition, and peptide binding properties of detergent soluble bilayers and detergent resistant rafts. *Biophys. J.* 82:1469–1482.
- Hao, Y. H., and J. W. Chen. 2001. Influence of cholesterol on the biophysical properties of the sphingomyelin/DOPC binary system. *J. Membr. Biol.* 183:85–92.
- Ipsen, J. H., G. Kalström, O. G. Mouritsen, H. W. Wennerström, and M. J. Zuckermann. 1987. Phase equilibria in the phosphatidylcholine-cholesterol systems. *Biochim. Biophys. Acta*. 905:162–172.
- Kahya, N., D. Scherfeldt, K. Bacia, B. Poolman, and P. Schwille. 2003. Probing lipid mobility of raft-exhibiting model membranes by fluorescence correlation spectroscopy. *J. Biol. Chem.* 278:28109–28115.
- Kärger, J., H. Pfeifer, and W. Heink. 1988. Principles and application of self-diffusion measurements by nuclear magnetic resonance. In *Advances in Magnetic and Optical Resonance*. W. S. Warren, editor. Academic Press, Inc., San Diego, CA. 1–89.
- Lawrence, J. C., D. E. Saslowsky, J. M. Edwardson, and R. M. Henderson. 2003. Real-time analysis of the effects of cholesterol on lipid raft behavior using atomic force microscopy. *Biophys. J.* 84:1827–1832.
- Leidy, C., T. Kaasgaard, J. H. Crowe, O. G. Mouritsen, and K. Jørgensen. 2002. Ripples and the formation of anisotropic lipid domains: imaging two-component supported double bilayers by atomic force microscopy. *Biophys. J.* 83:2625–2633.
- Lindblom, G., and G. Orädd. 1994. NMR studies of translational diffusion in lyotropic liquid crystals and lipid membranes. *Prog. NMR Spectrosc.* 26:483–515.
- Orädd, G., and G. Lindblom. 2003. NMR in macroscopically oriented lyotropic systems. In *NMR of Orientationally Ordered Liquids*. E. Burnell and K. de Lange, editors. Kluwer Academic Publishers, Dordrecht, The Netherlands. 399–418.
- Orädd, G., and G. Lindblom. 2004. NMR studies of macroscopically oriented bilayers. *Magn. Res. in Chem.* In press.
- Orädd, G., G. Lindblom, and P. W. Westerman. 2002. Lateral diffusion of cholesterol and DMPC in a lipid bilayer measured by pfg-NMR. *Biophys. J.* 83:2702–2704.
- Polson, J. M., I. Vattulainen, H. Zhu, and M. J. Zuckermann. 2001. Simulation study of lateral diffusion in lipid-sterol bilayer mixtures. *Eur. Phys. J. E*. 5:485–497.
- Rietveld, A., and K. Simons. 1998. The differential miscibility of lipids as the basis for the formation of functional membrane rafts. *Biochim. Biophys. Acta*. 1376:467–479.
- Rinia, H. A., M. M. Snel, J. P. van der Eerden, and B. de Kruijff. 2001. Visualizing detergent resistant domains in model membranes with atomic force microscopy. *FEBS Lett.* 501:92–96.
- Samsonov, A. V., I. Mihalyov, and F. S. Cohen. 2001. Characterization of cholesterol-sphingomyelin domains and their dynamics in bilayer membranes. *Biophys. J.* 81:1486–1500.
- Shaikh, S. R., A. C. Dumauual, L. J. Jenski, and W. Stillwell. 2001. Lipid phase separation in phospholipid bilayers and monolayers modeling the plasma membrane. *Biochim. Biophys. Acta*. 1512:317–328.
- Simons, K., and E. Ikonen. 1997. Functional rafts in cell membranes. *Nature*. 387:569–572.
- Simons, K., and D. Toomre. 2000. Lipid rafts and signal transduction. *Nat. Rev. Mol. Cell Biol.* 1:31–39.
- Simons, K., and G. van Meer. 1988. Lipid sorting in epithelial cells. *Biochemistry*. 27:6197–6202.
- Stilbs, P., and K. Paulsen. 1996. Global least-squares analysis of large, correlated spectral data sets. Application to chemical kinetics and time-resolved fluorescence. *Rev. Sci. Instrum.* 67:4380–4386.
- Stilbs, P., K. Paulsen, and P. C. Griffiths. 1996. Global least-squares analysis of large, correlated spectral data sets: application to component-resolved FT-PGSE NMR spectroscopy. *J. Phys. Chem.* 100:8180–8189.
- Tanner, J. E. 1970. Use of the stimulated echo in NMR diffusion studies. *J. Chem. Phys.* 52:2523–2526.
- Thewalt, J. L., and M. Bloom. 1992. Phosphatidylcholine: cholesterol phase diagrams. *Biophys. J.* 63:1176–1181.
- Tokumasu, F., A. J. Jin, G. W. Feigenson, and J. A. Dvorak. 2003. Nanoscopic lipid domain dynamics revealed by atomic force microscopy. *Biophys. J.* 84:2609–2618.
- Veatch, S. L., and S. L. Keller. 2002. Organization in lipid membranes containing cholesterol. *Phys. Rev. Lett.* 89:268101–1–268101–4.
- Veatch, S. L., and S. L. Keller. 2003. A close look at the canonical “raft mixture” in model membrane studies. *Biophys. J.* 84:725–726.
- Veiga, M. P., L. R. Arrondo, F. M. Goni, A. Alonso, and D. Marsh. 2001. Interaction of cholesterol with sphingomyelin in mixed membranes containing phosphatidylcholines, studied by spin-label ESR and IR spectroscopies. A possible stabilization of gel-phase sphingolipid domains by cholesterol. *Biochemistry*. 40:2614–2622.
- Vist, M. R., and J. H. Davis. 1990. Phase equilibria of cholesterol/dipalmitoylphosphatidylcholine mixtures: ^2H nuclear magnetic resonance and differential scanning calorimetry. *Biochemistry*. 29:451–464.
- Wästerby, P., G. Orädd, and G. Lindblom. 2002. Anisotropic water diffusion in macroscopically oriented lipid bilayers studied by pulsed magnetic field gradient NMR. *J. Magn. Reson.* 157:156–159.
- Yuan, C., J. Furlong, P. Burgos, and L. J. Johnston. 2002. The size of lipid rafts: an atomic force microscopy study of ganglioside GM1 domains in sphingomyelin/DOPC/cholesterol. *Biophys. J.* 82:2526–2535.